Supplementary information for Rapid metal pollutant deposition from the volcanic plume of Kīlauea, Hawai‘i (Ilyinskaya, Mason et al.)

Supplementary figures

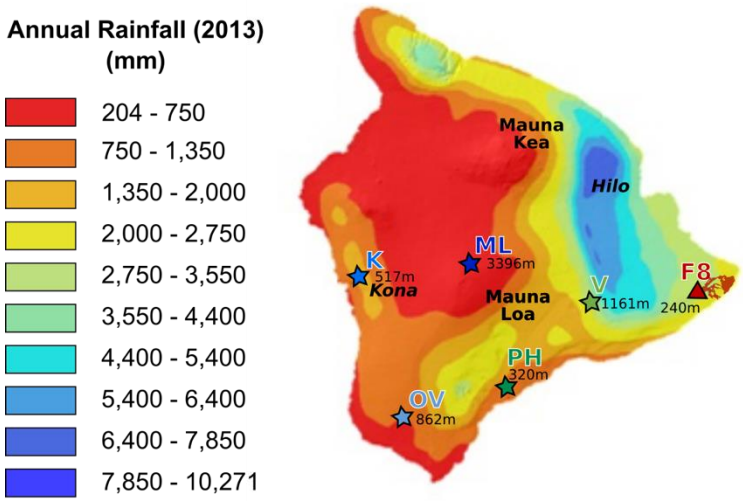

Supplementary Figure 1. Mean annual rainfall map adapted from the 2013 Rainfall Atlas of Hawai‘i.[17] Orographic lifting of persistent east-northeast trade winds gives rise to high mean rainfall on the windward mountain slopes, and low rainfall prevails in leeward lowlands and on the upper slopes of the highest mountains.

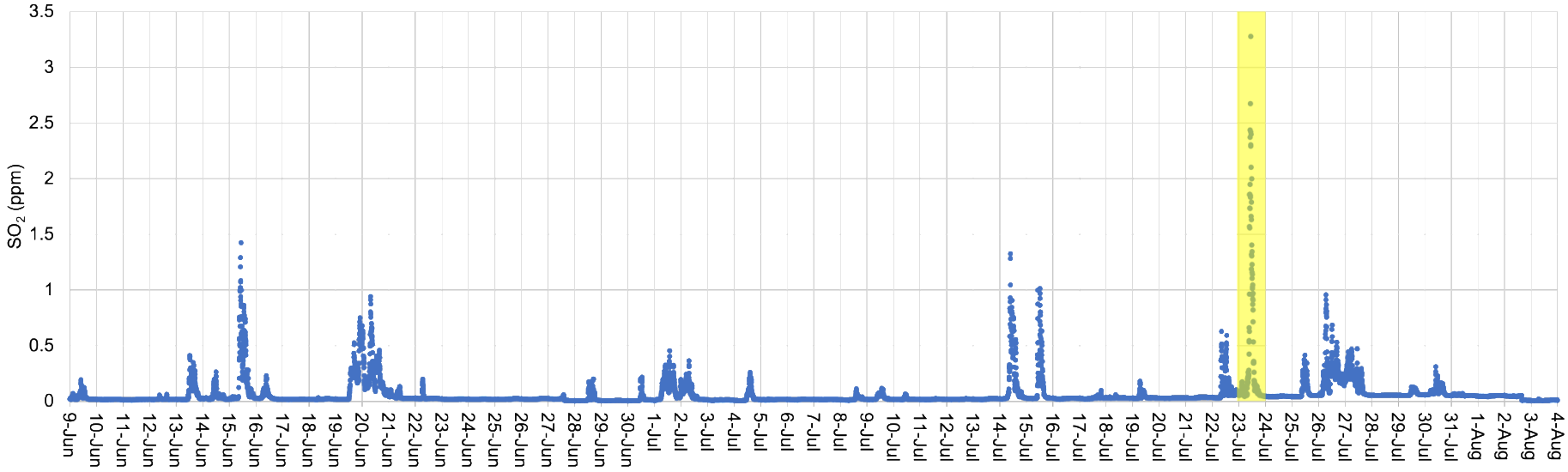

Supplementary Figure 2. Times series of SO_2 measured at Volcano Art Centre, from early June to the end of the main activity in 2018 on August 4th. Tick marks on the x axis mark midnight at the start of the date labelled. Our sampling period at Volcano village during the plume advection event is highlighted in yellow (23 July 2018). The time series shows that the advection event we captured during our sampling period for sample FP_07_01 was one of the strongest during the entire eruption, but also that such advection events were relatively common throughout the eruption, with no obvious periodicity.

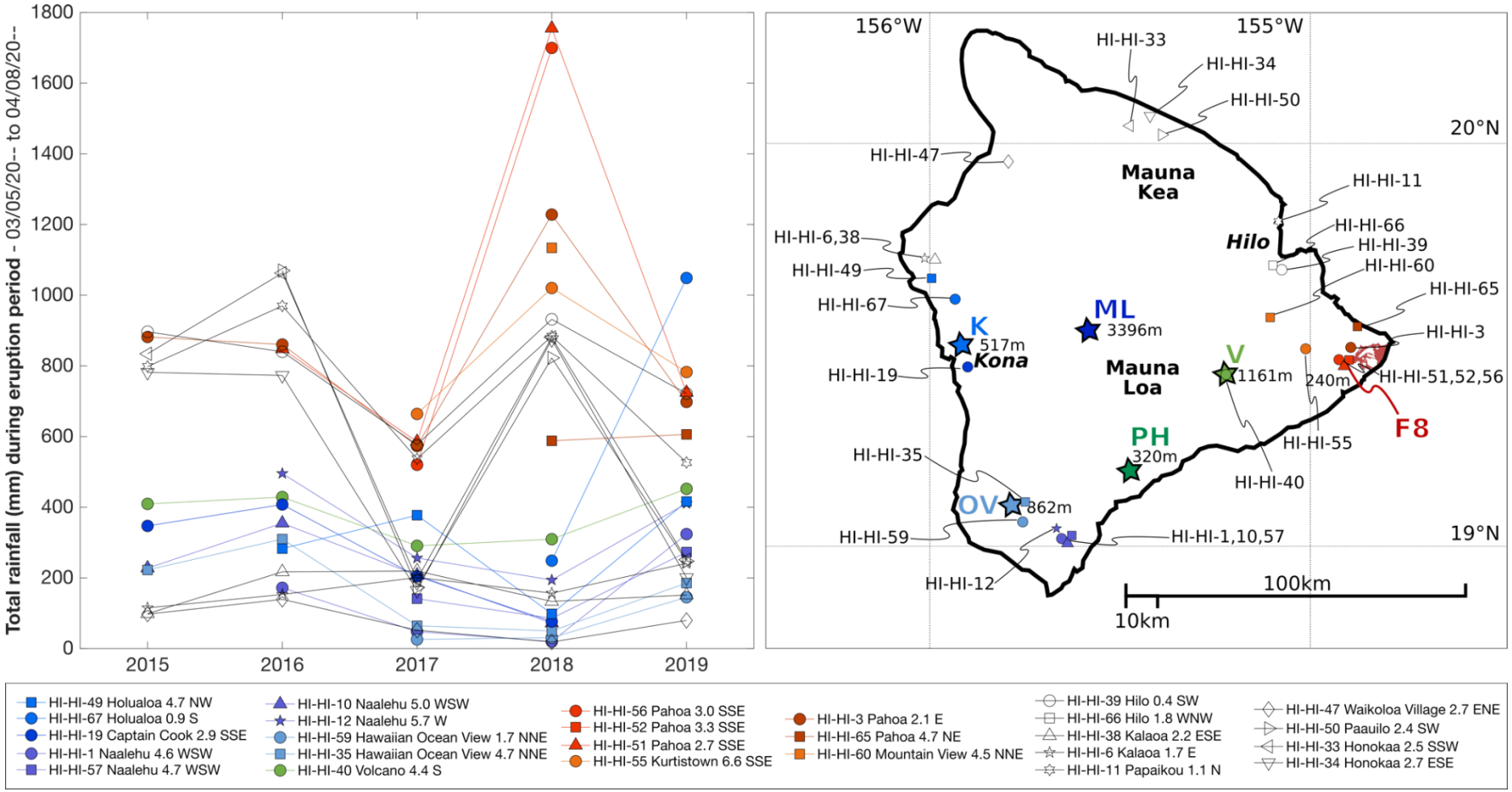

Supplementary Figure 3. CoCoRaHS community rainfall data collected at stations across the Island of Hawai'i. Note that data has not been collected continuously between 2015–2019, and some uncertainty may be introduced into this data due to inconsistent reporting of rainfall data. A longer time-series of rainfall data would be required to better assess whether 2018 was an statistically significant 'abnormal' year for rainfall over the Leilani Estates and Pahoa areas. For these reasons, this data is provided as 'anecdotal' evidence and was not included in the main paper.

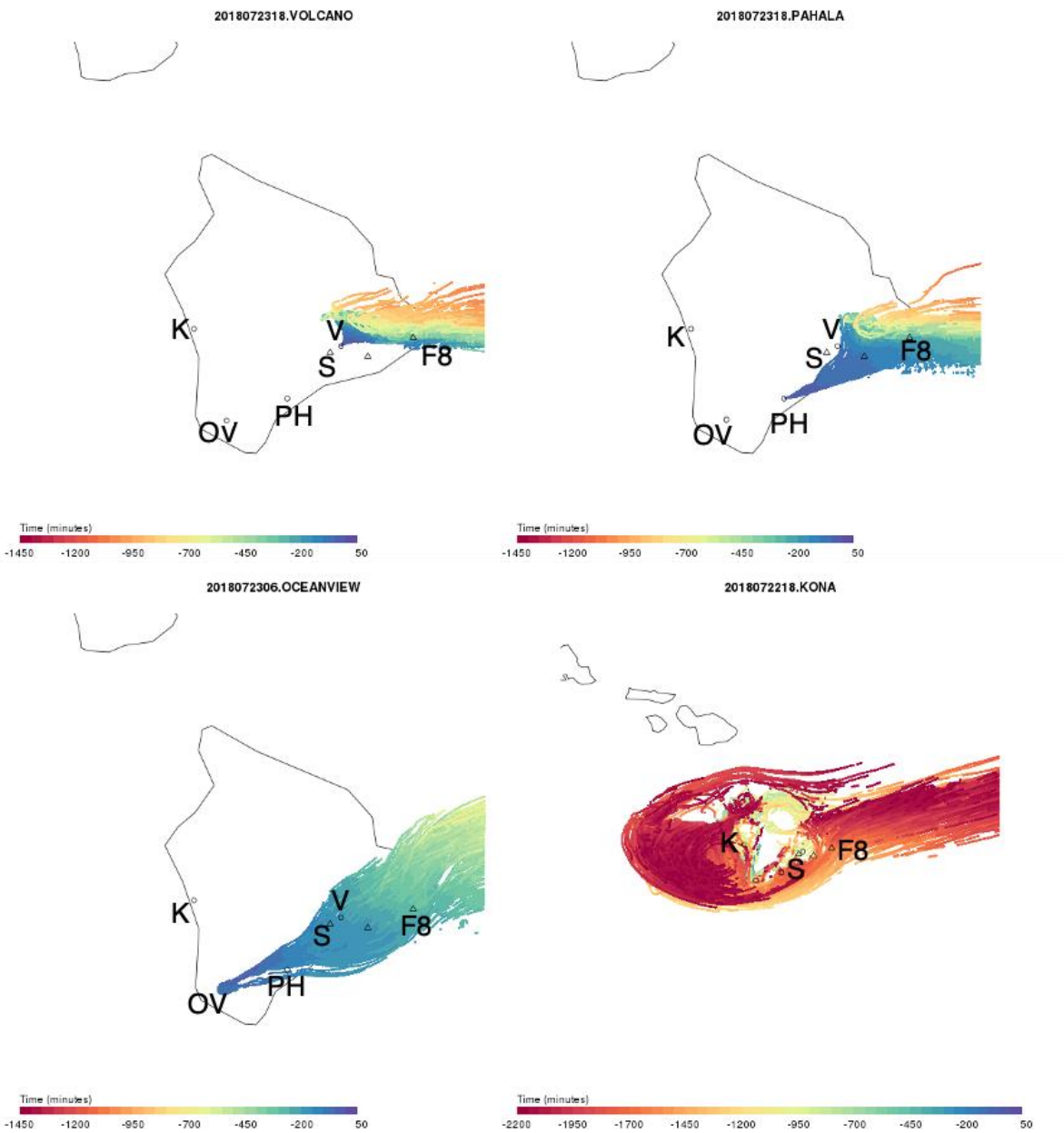

Supplementary Figure 4. Example of back-trajectory simulations where air parcels could be traced from a direct sampling site back to a volcanic emission source. The circles show the direct sampling sites from which back-trajectories were initiated: Volcano village (V), Pāhala (PH), Ocean View (OV) and Kailua-Kona (K). Triangles represent volcanic emission sources Fissure 8 (F8) and Kīlauea summit crater (S). The unlabeled triangle is Puʻu ʻŌʻō crater which was included in the simulations but inactive during the study period and therefore not included in the discussion. Trajectories which coincided between initialization location and emissions sources (within 3km) were considered in the calculations of plume age and plume path distance.

Supplementary Methods 1: Volcanic metal pollutant emission rates for Figure 1

Figure 1 in the paper presents a comparison between the rates of metal pollutant emissions from volcanoes and those from entire industrialized countries.

We note that the volcanic emission rates may not be sustained over as long time periods as the emissions from countries, however, we demonstrate that they can be significant point sources, and due to the typically sustained emissions (months to decades) of this set of basaltic volcanoes, at times their impact on the local environment in terms of the deposition of some trace metals, may be greater than some of the most polluting anthropogenic sources.

Volcanic metal pollutant emission rates are typically calculated using metal pollutant (X) to SO_2 ratios and SO_2 emission rates as follows:

$$Emission\ rate\ of\ X = \frac{X}{SO_2} * SO_2\ emission\ rate$$

Anthropogenic emission rates are taken directly from the sources references in Figure 1, i.e., they are not calculated in this study.

Supplementary Table 1. Details of volcanic emission sources shown on Figure 1

Volcano and date of sampling	**Source & date of SO_2 sampling**	**Source & date of metal pollutant sampling**	**Source and date of SO_2 emission rate sampling**
Kīlauea summit 2008	Mather et al. (2012)[1] – 21, 24, 25, July 2008	← same source and dates	HVO measurements 16–26 July 2008 (reported here: hvo.wr.usgs.gov)
Kīlauea LERZ 2018	Mason et al. (2021)[2], 24, 31 July 2018	← same source and dates	31 July 2018 (Mason et al., 2021)[2]; max sustained rate of ~200 kt/day (Kern et al. 2020)[3]
Holuhraun 2014	Gauthier et al. (2016)[4] – 2 October 2014	← same source and date	3-month averaged SO_2 flux (September-November 2014) from Gauthier et al. (2016)[4]
Etna 2001	Aiuppa et al. (2002)[5] – various dates, May to August 2001	Aiuppa et al. (2003)[6] – various dates, May to August 2001 (same as left)	Salerno et al. (2005)[7] – average emission rate for 2001 eruption
Stromboli 1993-1997	Allard et al. (2000)[8] – various dates in 1993, 1994, and 1997	← same source and dates	Daily mean emission rates from the same dates – Allard et al. (2000)[8] and references therein
Masaya 2000–01	Moune et al. (2010)[9] – samples from April 2000 and Jan-Feb 2001	← same source and dates	Average emission rates over sampling period (Moune et al., 2010[9], and references therein)
Ambrym 2007	Allard et al. (2016)[10] – October 13, 14, 25, 26 2007	← same source and dates	Allard et al. (2016)[10] – 8 October 2008

Supplementary Methods 2: SO_2 loss/S conversion rate

We can use our simultaneous measurements of SO_2 and SO_4^{2-} concentrations, and our estimates of plume age from back-trajectory plume dispersion simulations (**Methods M6**) to estimate the SO_2 loss rate.

We did not include this calculation in the main text both because it was not a focus of our work, and due to the large uncertainties and many caveats that must be considered when quantifying and comparing S conversion rates. We feel that a fully considered comparison of these rates in volcanic plumes requires further work and a more in-depth review than we have space for in this work. Some of the uncertainties and caveats are listed below.

- In our sampling, we only captured the SO_2 and SO_4^{2-} concentrations at ground level. Therefore, if sulphur species are stratified within the plume, as has been suggested at Kīlauea[11], this introduces substantial uncertainty into our SO_2 loss rate calculation.
- It is very important to consider the distance and time-period over which S conversion rates are calculated. When conversion/loss rates are averaged over entire days, this average rate will mask potentially orders of magnitude variability in the rate throughout the day (mainly due to changes in UV intensity). Changes in relative humidity and precipitation along the plume path will also change the rate of aqueous processing within the plume, which can accelerate the S conversion process.
- Also, along the plume path, SO_4^{2-} will be created through conversion from SO_2, but it will also be 'lost' (i.e., deposited) from the plume. Therefore, for conversion rates calculated over large distances, as ours from Fissure 8 to Kailua-Kona is below, loss of sulphate from the plume may lead to an inaccurate estimation of the actual S conversion rate in the plume. We note however, that despite these caveats, the rate may be useful for making rough estimates of the concentrations of sulphate communities downwind on the Island of Hawai'i might expect during subsequent eruptions.
- When comparing S conversion rates between studies, differences in methods, as well as differences in the time, distance and local atmospheric conditions during which the rate is quantified will all have an important impact on the calculated rate. These factors should be considered in detail when presenting any new conversion rates.

2.1. Methods for calculating the S conversion rate

The filter pack samples provided simultaneous measurements of SO_2 gas and SO_4^{2-} particulate matter concentrations, collected between the volcanic source (Fissure 8) and 3 downwind locations between 40 and 240 km distance (3-19hour plume age). This allowed a direct calculation to be made of sulphur gas-to-particle conversion rate. Note that samples collected at Pāhala were excluded from these calculations because they were saturated in SO_2 (**Supplementary Data 5**). The fraction of sulphur in the gas phase (X_S) was calculated as $X_S = [SO_{2(g)}]/([SO_{2(g)}]+[SO_4^{2-}{}_{(PM)}])$. X_S is shown as a function of plume age **Supplementary Figure 5**. The slope of the regression line through the observations yielded the sulphur gas-to-particle conversion rate: $2.8 \times 10^{-6} \pm 0.52 \times 10^{-6}$ s^{-1} (95% confidence interval). The calculation assumed that the proportions between $SO_{2(g)}$ and $SO_4^{2-}{}_{(PM)}$ were only affected by the gas-to-particle conversion rate; and that there was no preferential removal of one phase over the other from the plume. $SO_4^{2-}{}_{(PM)}$ can be highly water-soluble and hygroscopic and was likely preferentially removed via wet deposition compared to $SO_{2(g)}$; preferential removal of $SO_4^{2-}{}_{(PM)}$ will decrease the estimate of the conversion rate. The method also assumes that gas and PM are homogeneously distributed within the plume. However, it has been shown that SO_2 was sometimes concentrated at a higher altitude than PM using balloon-based vertical profiling during the 2018 eruption[11].

2.2. Results and discussion

The average empirical first-order rate constant for our ground-level conversion rate was calculated as $2.8 \times 10^{-6} \pm 0.4 \times 10^{-6}$ s^{-1} for July 2018 (equivalent to a mean SO_2 lifetime of ~4 days; **Supplementary Figure 5**), consistent with an independent estimate (using Hawai'i Department of Health air quality station data, also sampled at ground-level)[12] of $3.8 \times 10^{-6} \pm 1.3 \times 10^{-6}$ s^{-1} (mean SO_2 lifetime of ~3 days). Both of these rates are calculated using data that has been averaged over one or more days. Therefore the maximum SO_2 loss rate may be greater, depending on factors listed above[13]. The 2018 SO_2 loss rates above are an order of magnitude higher than the rate measured at Kīlauea in 2013 (5.3×10^{-7} s^{-1}), which did not take into account depositional processes and was measured during winter, where S conversion rates may be slower due to lower solar flux[14]. However, 2018 rates are within the range of rates reported from satellite measurements in 2008[15] (5.8×10^{-6} s^{-1} to 1.2×10^{-5} s^{-1}; SO_2 lifetime ~1–2 days), but are an order of magnitude lower than those made using ground-based measurements in 2001 (4.6×10^{-5} s^{-1}; SO_2 lifetime ~6 hours)[16].

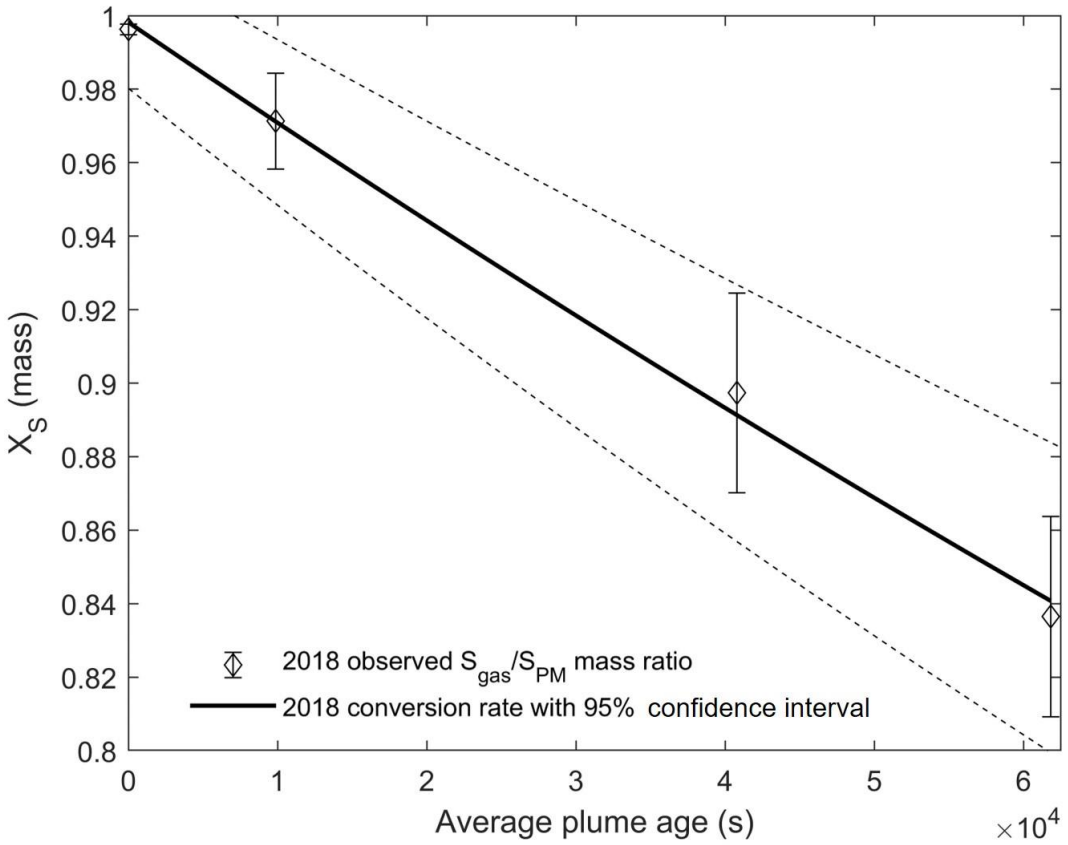

Supplementary Figure 5. X_S (mass) as a function of plume age (s). The y-error bars represent the standard deviation of all samples collected in each location. The gradient of a linear fit through the direct observations data gives a sulfur gas-to-particle conversion rate of $2.8 \times 10^{-6} \pm 0.52 \times 10^{-6}$ s^{-1} (95% confidence interval).

Supplementary references

1. Mather, T. A. *et al.* Halogens and trace metal emissions from the ongoing 2008 summit eruption of Kīlauea volcano, Hawai`i. *Geochim. Cosmochim. Acta* **83**, 292–323 (2012).

2. Mason, E. *et al.* Volatile metal emissions from volcanic degassing and lava-seawater interactions at Kīlauea Volcano, Hawai'i. *Commun. Earth Environ.* (accepted).

3. Kern, C. *et al.* Quantifying gas emissions associated with the 2018 rift eruption of Kīlauea Volcano using ground-based DOAS measurements. *Bull. Volcanol.* **82**, 55 (2020).

4. Gauthier, P.-J., Sigmarsson, O., Gouhier, M., Haddadi, B. & Moune, S. Elevated gas flux and trace metal degassing from the 2014–2015 fissure eruption at the Bárðarbunga volcanic system, Iceland. *J. Geophys. Res. Solid Earth* **121**, 1610–1630 (2016).

5. Aiuppa, A., Federico, C., Paonita, A., Pecoraino, G. & Valenza, M. S, Cl and F degassing as an indicator of volcanic dynamics: The 2001 eruption of Mount Etna. *Geophys. Res. Lett.* **29**, 54-1-54–4 (2002).

6. Aiuppa, A., Dongarrà, G., Valenza, M., Federico, C. & Pecoraino, G. Degassing of Trace Volatile Metals During the 2001 Eruption of Etna. *Volcanism Earths Atmosphere* (2003) doi:10.1029/139GM03.

7. Salerno, G., Caltabiano, T., Burton, M., Bruno, N. & Longo, E. Anomalous Degassing Rates From Mt. Etna, 2001-2005. *Geophys. Res. Abstr.* **7**, (2005).

8. Allard, P. *et al.* Acid gas and metal emission rates during long-lived basalt degassing at Stromboli Volcano. *Geophys. Res. Lett.* **27**, 1207–1210 (2000).

9. Moune, S., Gauthier, P.-J. & Delmelle, P. Trace elements in the particulate phase of the plume of Masaya Volcano, Nicaragua. *J. Volcanol. Geotherm. Res.* **193**, 232–244 (2010).

10. Allard, P. *et al.* Prodigious emission rates and magma degassing budget of major, trace and radioactive volatile species from Ambrym basaltic volcano, Vanuatu island Arc. *J. Volcanol. Geotherm. Res.* **322**, 119–143 (2016).

11. Vernier, J.-P. *et al.* VolKilau: Volcano rapid response balloon campaign during the 2018 Kilauea eruption. *Bull. Am. Meteorol. Soc.* (2020) doi:10.1175/BAMS-D-19-0011.1.

12. Whitty, R. C. W. *et al.* Spatial and Temporal Variations in SO2 and PM2.5 Levels from 2007-2018 Kīlauea Volcano, Hawai'i. *Front. Earth Sci.* **8**, 36 (2020).

13. Eatough, D. J., Caka, F. M. & Farber, R. J. The Conversion of SO2 to Sulfate in the Atmosphere. *Isr. J. Chem.* **34**, 301–314 (1994).

14. Kroll, J. H. *et al.* Atmospheric Evolution of Sulfur Emissions from Kīlauea: Real-Time Measurements of Oxidation, Dilution, and Neutralization within a Volcanic Plume. *Environ. Sci. Technol.* **49**, 4129–4137 (2015).

15. Beirle, S. *et al.* Estimating the volcanic emission rate and atmospheric lifetime of SO2 from space: a case study for Kīlauea volcano, Hawai`i. *Atmospheric Chem. Phys.* **14**, 8309–8322 (2014).

16. Porter, J. N. *et al.* Sun photometer and lidar measurements of the plume from the Hawaii Kilauea Volcano Pu'u O'o vent: Aerosol flux and SO2 lifetime. *Geophys. Res. Lett.* **29**, 30-1-30–4 (2002).

17. Giambelluca, T. W. *et al.* Online Rainfall Atlas of Hawai'i. *Bull. Am. Meteorol. Soc.* **94**, 313–316 (2013).